Space-dimension models of spectrum usage for cognitive radio networks

Miguel López-Benítez, *Member, IEEE,* Fernando Casadevall

***Abstract*—The Dynamic Spectrum Access (DSA) principle, relying on the Cognitive Radio (CR) paradigm, allows users to access spectrum over time intervals or spatial areas where it remains unused. Owing to the opportunistic nature of DSA/CR, the behaviour and performance of DSA/CR networks depends on the perceived spectrum usage pattern. An accurate modelling of spectrum occupancy therefore becomes essential in the context of DSA/CR. In this context, this work addresses the problem of accurately modelling the spectrum occupancy pattern perceived by DSA/CR users in the spatial domain. A novel spatial modelling approach is introduced in order to enable a simple yet practical and accurate characterisation of spectrum. First, a set of models are proposed to characterise and predict the average level of occupancy perceived by DSA/CR users at various locations based on the knowledge of some simple signal parameters. An extension is then proposed in order to characterise not only the average occupancy level but also the instantaneous channel state perceived simultaneously by DSA/CR users observing the same transmitter from different locations. The validity and accuracy of the theoretical models are demonstrated with results from an extensive spectrum measurement campaign. Some illustrative examples of their potential applicability are presented and discussed as well.**

***Index Terms*—Cognitive radio, dynamic spectrum access, spectrum occupancy models, spatial models.**

I. Introduction

COGNITIVE Radio (CR) has become one of the most intensively researched paradigms in radio communications [1]–[3]. A CR is a context-aware intelligent radio capable of autonomous reconfiguration by learning from and adapting to the surrounding radio environment. The two main defining features of a CR are its cognitive capability (ability to capture information and learn from the radio environment) and reconfigurability (ability to dynamically modify the transceiver parameters to adapt to varying communication conditions).

An important application of CR is Dynamic Spectrum Access (DSA) [3], [4], a concept that has been identified as a promising solution to enhance the overall efficiency of spectrum usage. Despite being a wider concept [5]–[7], DSA is often understood as an opportunistic spectrum access method whereby unlicensed (secondary) users are allowed to access, in a non-interfering manner, some licensed bands unoccupied by the licensed (primary) systems for a certain time period (time dimension) or over a certain area (spatial dimension). DSA/CR has been motivated by the outcomes of spectrum measurement campaigns performed all around the world [8]–[17], demonstrating that spectrum is underutilised. This indicates that new wireless systems based on DSA/CR can coexist with legacy systems in the same spectrum, leading to a more efficient exploitation of the available radio resources.

As a result of the opportunistic nature of DSA/CR, the behaviour and performance of secondary networks depend on the spectrum occupancy pattern of the primary system. Thus, the availability of realistic and accurate, yet simple spectrum occupancy models can provide significant benefits in DSA/CR research [18]. Spectrum usage models are frequently employed in the study of DSA/CR systems, ranging from analytical studies to the design and dimensioning of DSA/CR networks, including the development of new simulation tools and more efficient DSA/CR techniques. Spectrum usage models are also useful to determine the impact of DSA/CR systems on the performance of primary systems. This is particularly important for TV broadcasting systems given the fact that the initial deployments of DSA/CR networks are planned to take place in spectrum bands allocated to the TV broadcasting service.

This work focuses on the modelling of spectrum occupancy patterns in the spatial domain. Spatial spectrum opportunities arise when a spectrum band is exploited by the primary system within a bounded area, thus enabling the reuse of the same band by secondary users well outside this area (a clear example of this scenario is the spatial frequency planning of TV broadcasting systems). This work introduces a novel spatial modelling approach based on an innovative theoretical framework. The proposed models are envisaged to describe the average level of occupancy (expressed in terms of the channel duty cycle) perceived by DSA/CR users at various locations based on the knowledge of some simple primary signal parameters. Moreover, an extension is proposed in order to characterise not only the average spectrum occupancy but also the instantaneous busy/idle state perceived simultaneously by DSA/CR users observing the same transmitter from different locations. This extension can be useful in the study of cooperative techniques (e.g., cooperative spectrum sensing) as well as the development of innovative simulation tools. The validity and correctness of the theoretical models is evaluated

Manuscript received March 20, 2015; revised November 25, 2015, and February 4, 2016; accepted February 20, 2016. This work was supported by the Spanish Research Council under research project ARCO (Ref. TEC2010-15198) and the Spanish Ministry of Science and Innovation under FPU grant (Ref. AP2006-848).

M. López-Benítez is with the Department of Electrical Engineering and Electronics, University of Liverpool, Liverpool, United Kingdom (email: M.Lopez-Benitez@liverpool.ac.uk).

F. Casadevall is with the Department of Signal Theory and Communications, Universitat Politècnica de Catalunya, Barcelona, Spain (email: ferranc@tsc.upc.edu).

Color versions of one or more of the figures in this paper are available online at http://ieeexplore.ieee.org.

Digital Object Identifier 10.1109/TVT.2016.XXXXXXX

and corroborated with results from an extensive spectrum measurement campaign. Some illustrative examples of the potential applicability of these models are discussed as well.

In summary, the contributions of this work are as follows:

- This work provides, for various scenarios, closed-form relations between the average spectrum occupancy (in terms of the duty cycle) that would be observed by DSA/CR users at different locations and some simple operation parameters (received signal and noise powers, primary activity factors and false alarm probability).
- An extension is also developed to characterise not only the average spectrum occupancy observed in the long-term but also the instantaneous channel state perceived simultaneously by DSA/CR users observing the same transmitter from different locations.
- The validity and accuracy of the developed analytical models are corroborated with empirical data from an extensive spectrum measurement campaign.
- A discussion, with illustrative numerical results, is provided on how the developed models can be: i) combined with radio propagation models to provide a more realistic characterisation than the trivial busy/idle approach based on the average received power commonly considered in the literature, and ii) implemented in simulation tools to efficiently generate the spatial spectrum occupancy pattern perceived by DSA/CR users at different locations.

The rest of this work is organised as follows. First, Section II reviews previous related work. Section III then describes the methodology employed to capture and process the empirical data used in the validation of the proposed models, which are then presented in Section IV (models for average spectrum occupancy perception) and Section V (models for concurrent observations at different locations). The potential applicability of the developed models is illustrated in Section VI. Finally, Section VII summarises and concludes the work.

II. Previous work

The spatial dimension of spectrum occupancy has frequently been analysed and modelled in terms of the interference from a secondary network to a primary system as a function of relative locations, distances, transmission powers and radio propagation conditions [19]–[21]. Previous work has studied the aggregated interference from DSA/CR users surrounding a primary receiver [20], [22], [23], the outage probability of a primary system caused by the interference from a DSA/CR network for underlay and overlay spectrum sharing [24], the region of communication and interference for the users of a DSA/CR system that coexists with a cellular network [25], the interference to wireless microphones in TV bands [26], and refinements including shadowing and fading effects [27], [28] and power control in the secondary DSA/CR network [29].

This work deals with the modelling of the binary busy/idle occupancy state observed by DSA/CR users as a function of their spatial location. This relevant aspect has received less attention in DSA/CR research. For example, the spatial distribution of the spectral occupancy was analysed in [30] in the context of a cellular mobile communication system. In contrast to other similar works where a cellular network is monitored by means of external field measurements and in a limited geographical region [31]–[33], the study reported in [30] monitors the arrival of calls inside an operator's network and simultaneously over hundreds of base stations over the period of 3 weeks. Based on such measurements and making use of variograms, [30] analyses the spatial variability of spectrum occupancy for sectors of the same and different cells as well as the correlation among various cells based on the traffic supported during the minute of maximum load. Although the analyses in [30] show interesting spatial properties of spectrum use in cellular systems, no model enabling the reproduction of the analysed statistics and patterns is developed.

The possibility to characterise spectrum occupancy in the spatial domain by means of spatial statistics and random fields is explored in [34]. Based on the spatial statistics studied in [34], a modelling procedure is proposed in [35] and complemented in [36]. The procedure in [35], [36] consists in determining the average power over a set of points in a specified geographical area, with a certain spatial distribution. This information can be obtained by means of field measurements (empirical model [35]) or simulators and radio planning software tools (deterministic model [36]). Once the spatial values of average power are determined, the resulting values are employed to fit an analytic semivariogram model, which permits reproduce the statistical properties of the average powers observed over a certain region.

Some related studies have appeared more recently. A 3-dimensional analytical interference model is proposed in [21], which is used to determine the number of TV channels available for secondary DSA/CR users in different indoor locations. An alternative modelling approach is developed in [37], where a framework for the statistical estimation of primary transmitter locations is proposed based on the spatial characterisation of spectrum usage in a collaborative spectrum sensing context. Several joint time-space studies have been published as well. A study on the impact of time-domain primary activity parameters (distributions of on/off holding times) on the opportunities of spatial spectrum reuse is presented in [38] along with a discussion on simple models for occurrences of spectrum opportunities over both time and space. In [39], the theory of random fields is applied to the modelling of spatial-temporal correlated spectrum usage data. A theoretical analysis on the probability distribution of wireless signal strength received from mobile stations is performed in [40], where a polylogarithm-like statistical model to characterise the spatio-temporal dynamics of the mobile service spectrum usage is proposed. A more detailed review of spectrum occupancy models for CR can be found in [41].

While spectrum occupancy modelling in the time and frequency domains has received a great deal of attention, spectrum modelling in the space domain has received significantly less attention. This work develops a novel theoretical spatial modelling framework, validated with empirical data, to characterise the binary busy/idle occupancy patterns observed by DSA/CR users as a function of their spatial location, based on the knowledge of simple signal parameters.

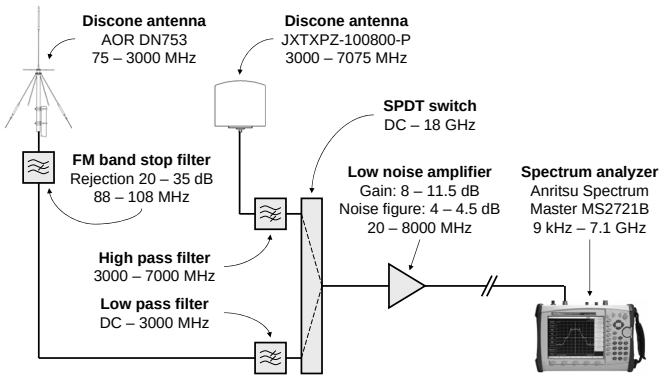

Fig. 1. Measurement platform employed in this work.

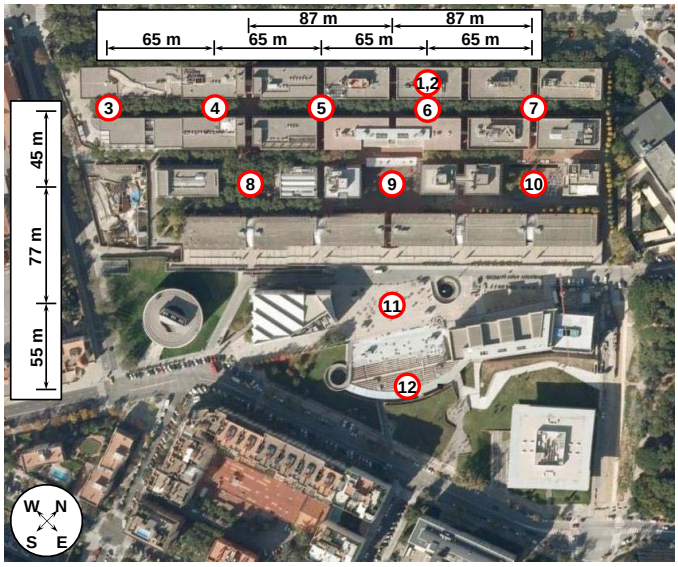

Fig. 2. Measurement locations considered in this work.

III. Measurement Setup and Methodology

The measurement platform employed in this work is depicted in Fig. 1. The design is composed of two discone antennas (75-7075 MHz), a Single-Pole Double-Throw (SPDT) switch to select the desired antenna, several filters to remove out-of-band and overloading FM signals, a low-noise preamplifier to enhance the overall sensitivity, and a high performance spectrum analyser to record the spectral activity. The spectrum analyser is connected to a laptop via Ethernet and controlled by a tailor-made software based on the Matlab's Instrument Control Toolbox. A GPS receiver is connected to the laptop via USB to provide a unique time reference for simultaneous synchronised measurements. The captured power samples are compared to a decision threshold, following an energy detection method [42], in order to extract binary busy/idle channel occupancy patterns. A detailed description of the measurement platform design and configuration and associated methodological aspects can be found in [43], [44].

The spectral activity of a wide variety of spectrum bands and radio technologies was monitored, including broadcasting systems such as analog TV, digital TV and Digital Audio Broadcasting (DAB) as well as amateur systems, paging systems, Private/Public-Access Mobile Radio (PMR/PAMR) systems such as TETRA, and cellular mobile communication systems such as GSM 900, DCS 1800 and UMTS FDD. Measurements were performed over a set of strategically selected locations in a urban environment (see Fig. 2), including an outdoor high point in a building rooftop with direct line-of-sight to several transmitters a few tens or hundreds of meters apart (location 1), indoor environments (location 2), and additional outdoor locations in narrow streets (locations 3-7), between buildings (locations 8-10) and open areas (locations 11-12). For more details, the reader is referred to [45]. The considered measurement locations represent various scenarios of practical interest and embrace a wide range of receiving conditions and levels of radio propagation blocking, ranging from direct line of sight to severely blocked and faded signals. This variety of measurement conditions allowed the same transmitters to be observed under different radio propagation conditions and Signal-to-Noise Ratio (SNR) levels.

Two different types of measurements were performed. First, each location in Fig. 2 was measured individually in order to determine the perceived average occupancy as a function of the experienced SNR. This information was used to validate the models for average spectrum occupancy perception presented in Section IV. Afterwards, two identical measurement suites were employed for simultaneous synchronised measurements. One measurement suite was placed in the outdoor high point (location 1 in Fig. 2), where the receiving SNR was observed to be maximum for the analysed bands, while the second measurement suite was displaced along the rest of outdoor measurement locations at the ground level (locations 3-12 in Fig. 2), performing concurrent measurements for every possible pair of locations. These measurements provided information about how the instantaneous occupancy of a certain band is perceived at different locations. This information was used to validate the models for concurrent observations presented in Section V. The empirical data captured for various radio technologies enabled an adequate validation of the theoretical models developed in this work.

IV. Models for Average Perception

This section presents a set of spectrum occupancy models envisaged to characterise the average spectrum occupancy perceived at different locations in terms of the channel Duty Cycle (DC). The interest of employing the DC lies in its ability to summarise, in a single numerical value, the overall spectrum occupancy within a certain time interval and frequency range. The DC has been employed in past spectrum utilisation studies to quantify and compare the occupancy level of various spectrum bands, or the same band under different conditions or at different locations. The DC is employed in this work as a means to describe the spectrum occupancy level perceived by DSA/CR terminals at different locations.

It is worth making a clear distinction between the Activity Factor (AF) of a primary transmitter and the DC perceived by secondary terminals. The AF of a primary transmitter represents the fraction of time (or probability) that the transmitter is active (i.e., transmitting in the channel), while the DC of a

channel can be defined as the fraction of time (or probability) that the channel is observed as busy. A DSA/CR terminal in an arbitrary location with good radio propagation conditions with respect to the primary transmitter would observe the channel as busy whenever the primary transmitter is active. In such a case, the observed DC would be equal to the AF of the transmitter. However, at other locations where the propagation conditions are not so favourable, the primary signal might not be detected always. In such another case, the level of spectrum activity perceived by the DSA/CR terminal in terms of the DC would be lower than the actual AF of the primary transmitter. While the AF is unique for a given transmitter, the DC perceived at different locations may be different. Since the propagation conditions strongly vary with the location, the perceived DC will vary over space accordingly. The aim of this section is to develop models capable to describe the DC perceived at various locations as a function of the received signal strength.

A. Distribution of the received average power

The channel state perceived by a DSA/CR user (busy or idle) depends, among other factors, on the employed spectrum sensing method. Due to its simplicity, wide range of application and relevance, energy detection [42] has been the preferred spectrum sensing method for DSA/CR and is also considered in this work. According to the energy detection method, a DSA/CR terminal measures the power received in a frequency band over a time interval $2T$, which can be expressed as:

$$P_R = \frac{1}{2T} \int_{-T}^{+T} P_R(t)\, dt \qquad (1)$$

where $P_R(t)$ is the instantaneous power received by the DSA/CR terminal (including noise) and P_R is the average power employed as a test statistic to decide whether a primary signal is present in the sensed channel. The spectrum occupancy perception of a DSA/CR user at a particular location depends on the statistics of the received average power, P_R, which in turn depends on the radio propagation conditions resulting from the surrounding environment. The perceived spectrum occupancy can therefore be related to the received average power and analysed based on the statistics of P_R, which can be inferred as follows.

The Probability Density Function (PDF) of $P_R(t)$ is in general unknown since it is the result of the combined effects of the primary transmission power pattern, which can be assumed to be unknown to a secondary terminal, and the radio propagation mechanisms. However, the instantaneous power $P_R(t)$ is a stochastic process[1] that can be thought of as a non-countable infinity of independent and identically distributed random variables, one for each time instant t. As P_R is obtained by averaging an infinite number of random variables, the central limit theorem can be employed to approximate the PDF of P_R with a Gaussian/normal distribution, regardless of the particular distribution of the instantaneous power $P_R(t)$.

[1]Note that even if the primary transmission power is perfectly constant, the radio propagation channel results in some random variation of the received power $P_R(t)$. Moreover, the unavoidable effects of the receiver's noise also result in some random component in $P_R(t)$.

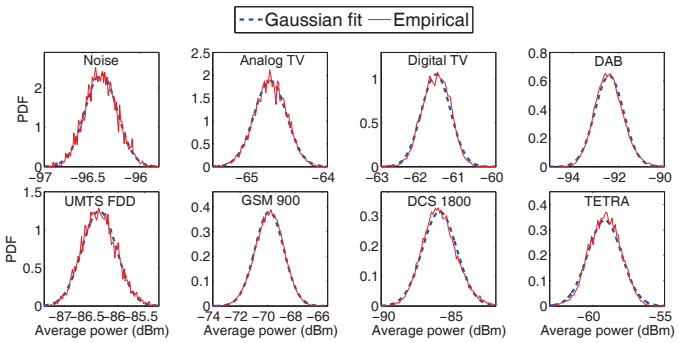

Fig. 3. Validation of the Gaussian approximation for the PDF of the received average power.

The validity of the Gaussian approximation is verified in Fig. 3 for signals of various radio technologies and the thermal noise's average power (measured by replacing the antenna with a matched load). It is worth noting that the power samples provided by swept spectrum analysers are obtained by sequentially tuning a narrowband filter to a set of consecutive frequency points. Every frequency point is measured for a certain time interval, thus causing some unavoidable averaging effect over the measured signal. Therefore, due to the inherent operating principle, the power values provided by spectrum analysers implicitly include the averaging effect of (1). Fig. 3 compares the distribution of the P_R values captured by the spectrum analyser at some selected channels[2] and the Gaussian curve corresponding to the sample mean and sample variance of the P_R values. Although signals from different radio technologies received at different frequencies are expected to exhibit various instantaneous power patterns $P_R(t)$, Fig. 3 indicates that in the considered problem the received average power P_R can be modelled as a Gaussian random variable for all cases regardless of the particular instantaneous power distributions, thus verifying the formulated hypothesis. Notice the analogy between the average power P_R and the test statistic of an energy detector, which is frequently modelled as a Gaussian random variable [46].

B. Spatial duty cycle models

This section develops a set of generic spectrum occupancy models to characterise and predict[3], based on the statistics of the received average power, the average occupancy level perceived by DSA/CR users in terms of the channel DC (a preliminary version was presented in [47]).

Let's denote the noise power distribution as $f_N(P_N) \sim \mathcal{N}(\mu_N, \sigma_N^2)$ and the signal power distribution (received in the presence of noise) as $f_S(P_S) \sim \mathcal{N}(\mu_S, \sigma_S^2)$. According to this formulation, μ_N represents the noise floor of the DSA/CR

[2]Spectrum analysers normally provide power measurements in logarithmic magnitudes (e.g., dBm). For convenience, to simplify the validation with field measurements, it is assumed hereinafter that all power values, means and variances are in logarithmic magnitude.

[3]In this work the term *prediction* of the duty cycle refers to the calculation of the observed duty cycle based on the set of parameters it depends on (i.e., given the particular operation conditions, the aim is to determine the corresponding duty cycle that would be observed by a DSA/CR user under such conditions).

receiver and σ_N denotes the standard deviation of the noise powers P_N experienced at various sensing events (the effective noise power may vary between sensing events due to the finite averaging period T or other reasons such as temperature variations). The primary power P_S received in the presence of noise is characterised by an average value μ_S that depends on the transmission power and propagation attenuation, and a standard deviation σ_S that is additionally affected by the DSA/CR receiver's noise.

Assuming energy detection, a DSA/CR terminal will report the sensed channel as busy whenever the observed average power is above a certain decision threshold λ. Since energy detection is not able to distinguish between intended signals and undesired noise, the channel will be reported as busy not only when a primary signal is received above the decision threshold, but also when there is no signal (or it is received below the threshold) and the noise power exceeds the level λ.

When a sensed channel is idle, the PDF of the observed average power, $f_R(P_R)$, will be that of the noise, $f_N(P_N)$, and the probability that the observed power is above the threshold (i.e., the perceived DC, Ψ) is given by (see Fig. 4):

$$\Psi_{idle} = \int_{\lambda}^{\infty} f_R(P_R) dP_R = \int_{\lambda}^{\infty} f_N(P_N) dP_N = P_{fa} \quad (2)$$

where it is assumed that the decision threshold λ is set so as to meet a specified probability of false alarm P_{fa}.

On the other hand, if the channel is busy when it is sensed, the PDF of the observed average power, $f_R(P_R)$, will be that of the received signal, $f_S(P_S)$. Assuming an ideal situation where there is no noise, the DC perceived by the DSA/CR user would be given by:

$$\begin{aligned}\Psi_{busy}^{ideal} &= \int_{\lambda}^{\infty} f_R(P_R) dP_R = \int_{\lambda}^{\infty} f_S(P_S) dP_S \\ &= \frac{1}{\sqrt{2\pi}\sigma_S} \int_{\lambda}^{\infty} e^{-\frac{1}{2}\left(\frac{P_S-\mu_S}{\sigma_S}\right)^2} dP_S = \mathcal{Q}\left(\frac{\lambda-\mu_S}{\sigma_S}\right)\end{aligned} \quad (3)$$

where $\mathcal{Q}(\cdot)$ represents the Gaussian Q-function [48, (26.2.3)]. Notice that (3) indicates that the perceived occupancy in terms of the DC would tend to zero as the received signal power P_S decreases (i.e., $\lim_{\mu_S \to -\infty} \Psi_{busy}^{ideal} = 0$). However, if the received signal power is below the receiver's noise, this situation would be equivalent to an idle channel where the receiver observes noise. In such a case, the actually perceived DC would be P_{fa}, instead of zero, as indicated by (2). A more realistic model for $f_R(P_R)$ when the channel is busy, taking into account the presence of noise, would be $f_R(P_R) = \mathcal{M}\{f_N(P_N), f_S(P_S)\}$, where $\mathcal{M}\{\cdot\}$ denotes a *realisation-wise maximum operator* defined as follows. If $\mathcal{A} = \{x_{a_1}, x_{a_2}, \ldots, x_{a_n}, \ldots, x_{a_N}\}$ and $\mathcal{B} = \{x_{b_1}, x_{b_2}, \ldots, x_{b_n}, \ldots, x_{b_N}\}$ represent two sets of N random numbers (realisations of a random variable) following PDFs $f_a(x_a)$ and $f_b(x_b)$, respectively, then $f_c(x_c) = \mathcal{M}\{f_a(x_a), f_b(x_b)\}$ represents the PDF of the elements of the set $\mathcal{C} = \{x_{c_1}, x_{c_2}, \ldots, x_{c_n}, \ldots, x_{c_N}\}$, where $x_{c_n} = \max\{x_{a_n}, x_{b_n}\}$ for $n = 1, 2, \ldots, N$, when N tends towards infinity. Note that this operator reproduces the effect of the noise floor on the observed power levels (i.e., the DSA/CR user observes the received signal power P_S when it is above the noise floor, or the noise power P_N otherwise). Therefore, this definition of $f_R(P_R)$ provides a more realistic model for the average power P_R actually observed by a real radio receiver. Based on this model, the DC perceived by the DSA/CR user when the channel is busy will then be given by:

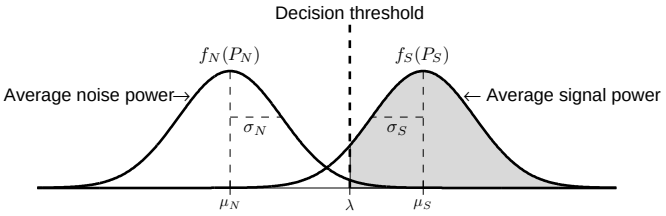

Fig. 4. Model for computing the DC (shaded area).

$$\begin{aligned}\Psi_{busy}^{real} &= \int_{\lambda}^{\infty} f_R(P_R) dP_R \\ &= \int_{\lambda}^{\infty} \mathcal{M}\{f_N(P_N), f_S(P_S)\} dP_R \\ &\approx \max\left\{\int_{\lambda}^{\infty} f_N(P_N) dP_N, \int_{\lambda}^{\infty} f_S(P_S) dP_S\right\} \\ &= \max\left\{P_{fa}, \mathcal{Q}\left(\frac{\lambda-\mu_S}{\sigma_S}\right)\right\}\end{aligned} \quad (4)$$

As appreciated, this model rightly predicts that the probability to observe a channel as busy is never lower than the target P_{fa}, as it occurs in a real radio receiver.

The average DC perceived by a DSA/CR user depends on the primary transmission power and particular activity pattern. The following sections provide closed-form expressions for various particular cases[4].

1) Constant-power continuous transmitters: This section considers the case of constant-power primary transmitters with an AF of 100% (e.g., TV and DAB). This case provides the basis for a simple model that will be extended in the next sections for variable-power and/or discontinuous transmitters.

If the primary transmitter is always active, the PDF of the received average power $f_R(P_R)$ will be that of the primary signal (with noise) at the location of the DSA/CR terminal, i.e., $f_R(P_R) = \mathcal{M}\{f_N(P_N), f_S(P_S)\}$. The probability that the received average power P_R is above the decision threshold λ and the DSA/CR user observes the channel as busy is given by (4). Assuming that the decision threshold is set so as to meet a certain target P_{fa}:

$$\begin{aligned}P_{fa} &= \int_{\lambda}^{\infty} f_N(P_N) dP_N = \frac{1}{\sqrt{2\pi}\sigma_N} \int_{\lambda}^{\infty} e^{-\frac{1}{2}\left(\frac{P_N-\mu_N}{\sigma_N}\right)^2} dP_N \\ &= \mathcal{Q}\left(\frac{\lambda-\mu_N}{\sigma_N}\right)\end{aligned} \quad (5)$$

Solving (5) for λ yields the decision threshold:

$$\lambda = \mathcal{Q}^{-1}(P_{fa})\,\sigma_N + \mu_N \quad (6)$$

[4]Preliminary versions of these models were published in [47] based on the ideal noise-free case of (3). More realistic versions based on (4) are presented in this section.

where $\mathcal{Q}^{-1}(\cdot)$ denotes the inverse of $\mathcal{Q}(\cdot)$. Substituting (6) into (4) finally yields the DC model:

$$\Psi = \max\left\{P_{fa}, \mathcal{Q}\left(\frac{\mathcal{Q}^{-1}(P_{fa})\,\sigma_N - \Gamma}{\sigma_S}\right)\right\} \quad (7)$$

where $\Gamma = \mu_S - \mu_N$ is the average SNR expressed in decibels, while σ_S and σ_N are the standard deviation of the signal and noise average powers also in decibels.

2) Constant-power discontinuous transmitters: This section extends the model of (7) by including the case of constant-power but non-continuous transmitters. If the primary transmitter is characterised by a certain AF, denoted as $0 < \alpha < 1$, the PDF of the received average power $f_R(P_R)$ will be that of the primary signal (with noise) $\mathcal{M}\{f_N(P_N), f_S(P_S)\}$ whenever the transmitter is active (which will occur with probability α) or noise $f_N(P_N)$ otherwise. Hence:

$$f_R(P_R) = (1-\alpha)\, f_N(P_N) + \alpha\, \mathcal{M}\{f_N(P_N), f_S(P_S)\} \quad (8)$$

and the resulting expression for the DC becomes:

$$\begin{aligned}
\Psi &= \int_\lambda^\infty f_R(P_R) dP_R \\
&= (1-\alpha)\int_\lambda^\infty f_N(P_N) dP_N \\
&\quad + \alpha \int_\lambda^\infty \mathcal{M}\{f_N(P_N), f_S(P_S)\}\, dP_R \\
&\approx (1-\alpha)\int_\lambda^\infty f_N(P_N) dP_N \\
&\quad + \alpha\, \max\left\{\int_\lambda^\infty f_N(P_N) dP_N, \int_\lambda^\infty f_S(P_S) dP_S\right\} \\
&= (1-\alpha) P_{fa} + \alpha\, \max\left\{P_{fa}, \mathcal{Q}\left(\frac{\mathcal{Q}^{-1}(P_{fa})\,\sigma_N - \Gamma}{\sigma_S}\right)\right\}
\end{aligned} \quad (9)$$

which reduces to (7) for $\alpha = 1$.

3) Variable-power discontinuous transmitters: In the case of variable-power transmitters, the average transmission power is not constant, but characterised by a certain PDF instead. To simplify the model, let's assume that the primary transmission power pattern can adequately be characterised by a discrete set of K average transmission power levels, instead of a continuous PDF. This assumption not only simplifies the resulting analytical expressions of the model, but also allows the application of the model to those cases where a channel is time-shared by K transmitters, transmitting at different average power levels, as it may be the case of various TDMA-based systems such as GSM/DCS, TETRA, etc. This approach embraces the case of a single variable-power transmitter with K transmission power levels, the case of K constant-power transmitters time-sharing the channel, or a combination of both. In any case, the problem reduces to the possibility of observing K average received powers in the channel.

Let's denote as $f_{S_k}(P_{S_k})$, with mean μ_{S_k} and standard deviation σ_{S_k}, the PDF of the received average power when the k-th average transmission power is selected ($k = 1, 2, \ldots, K$). Let's define an AF α_k for each transmission power representing the fraction of time (or probability) that the k-th transmission power is selected. In the case of a single-transmitter with K transmission power levels, only one out of the K power levels can be selected at a time. Moreover, in the case of K transmitters time-sharing the channel it is reasonable to assume that there exists some MAC mechanism so that when one primary transmitter accesses the channel the rest of potential primary transmitters remain inactive. In both cases, the K average power levels are mutually exclusive, and hence $\sum_{k=1}^K \alpha_k \leq 1$, where the equality holds when the channel is always busy. The left-hand side of the inequality represents the probability that any of the K transmitters is active (and the channel is busy), and its complementary probability $1 - \sum_{k=1}^K \alpha_k$ is the probability that the channel is idle. The PDF of the received average power $f_R(P_R)$ will be that of the k-th primary signal (with noise) $\mathcal{M}\{f_N(P_N), f_{S_k}(P_{S_k})\}$ whenever the k-th transmission power is active (which will occur with probability α_k) or it will be noise $f_N(P_N)$ otherwise. Hence:

$$\begin{aligned}
f_R(P_R) = &\left(1 - \sum_{k=1}^K \alpha_k\right) f_N(P_N) \\
&+ \sum_{k=1}^K \alpha_k\, \mathcal{M}\{f_N(P_N), f_{S_k}(P_{S_k})\}
\end{aligned} \quad (10)$$

and the resulting expression for the DC becomes:

$$\begin{aligned}
\Psi &= \int_\lambda^\infty f_R(P_R) dP_R \\
&= \left(1 - \sum_{k=1}^K \alpha_k\right) \int_\lambda^\infty f_N(P_N) dP_N \\
&\quad + \sum_{k=1}^K \alpha_k \int_\lambda^\infty \mathcal{M}\{f_N(P_N), f_{S_k}(P_{S_k})\}\, dP_R \\
&\approx \left(1 - \sum_{k=1}^K \alpha_k\right) P_{fa} \\
&\quad + \sum_{k=1}^K \alpha_k \max\left\{P_{fa}, \mathcal{Q}\left(\frac{\mathcal{Q}^{-1}(P_{fa})\,\sigma_N - \Gamma_k}{\sigma_{S_k}}\right)\right\}
\end{aligned} \quad (11)$$

where $\Gamma_k = \mu_{S_k} - \mu_N$ is the SNR resulting from the k-th average transmission power level expressed in decibels.

C. Model validation

This section validates with empirical data the models presented in Section IV-B. Note that the models of Sections IV-B1 and IV-B2 are particular cases of the model of Section IV-B3, with (11) reducing to (9) for $K = 1$ and $\alpha < 1$, and (7) for $K = 1$ and $\alpha = 1$. Thus, the validation of the general form of (11) also validates the particular cases of (7) and (9).

Fig. 5 shows the PDF of the received power for a time-shared channel where two transmitters ($K = 2$) are present. The left-most Gaussian bell corresponds to the noise of the channel, which was measured by replacing the antenna of the measurement platform with a matched load. The captured noise samples were used to estimate the noise parameters (μ_N, σ_N), which are used to depict the noise distribution $f_N(P_N)$ shown in Fig. 5. The other two Gaussian bells correspond to the two signals present in the channel. Note that all the received signal powers are well above the noise and both

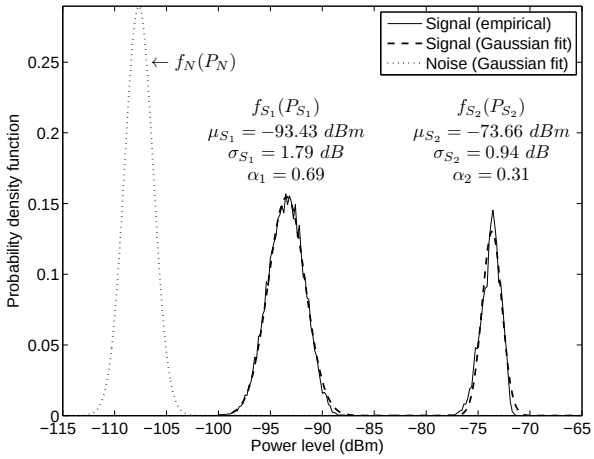

Fig. 5. Empirical and fitted PDF of the received power for a time-shared channel (two signals are present).

signals are far enough from each other to reliably classify the captured signal samples (e.g., samples below -85 dBm belong to the first signal and samples above -80 dBm belong to the second signal). Based on this observation, two signal sequences S_k ($k \in \{1, 2\}$) can be extracted from the captured samples. These sequences were used to estimate the signal parameters (μ_{S_k}, σ_{S_k}, α_k), which are used to depict, based on (10), the fitted signal distributions $f_{S_k}(P_{S_k})$ in Fig. 5.

The DC model is validated as follows. The two extracted signal sequences S_k are individually processed to simulate the received signals S_k at arbitrary SNR levels. This is accomplished by substracting the adequate amplitude value from the samples of the sequences S_k so as to meet the desired SNR, given by $\Gamma_k = \mu_{S_k} - \mu_N$. As signal amplitudes below the noise floor cannot be detected and are reported as noise, samples lying below the noise floor after subtracting the adequate amplitude value are replaced with a random noise level drawn from a Gaussian distribution with appropriate mean μ_N and standard deviation σ_N. Various combinations of SNR values for the signal components, (Γ_1, Γ_2), are simulated, and the resulting signal is compared to a decision threshold in order to determine the corresponding DC. The obtained empirical-simulated results for decision thresholds corresponding to target P_{fa} values of 1% and 10% are shown in Figs. 6(a) and 6(d), respectively. The DC corresponding to each simulated pair (Γ_1, Γ_2) was also predicted based on (11), making use of the estimated parameters (μ_{S_k}, σ_{S_k}, α_k) shown in Fig. 5. The theoretical predictions are shown in Figs. 6(b) and 6(e) for target P_{fa} values of 1% and 10%, respectively. The differences between the empirical-simulated and theoretically predicted DC values are shown in Figs. 6(c) and 6(f) for the considered target P_{fa} values. As appreciated, the maximum absolute error for P_{fa} = 1% is below 1.5%, while the value of the same parameter for P_{fa} = 10% is below 8%. These results not only corroborate the ability of the developed model to predict the average DC perceived by a DSA/CR user based on some basic signal parameters, but also demonstrate the accuracy attained with the proposed modelling approach.

V. Models for concurrent observations

The models developed in Section IV describe the average level of spectrum occupancy (expressed in terms of the DC) perceived by DSA/CR users at a specified location. In the study of spatial DSA/CR, it can be useful to characterise not only the average level of perceived spectrum occupancy, but also the simultaneous observations of DSA/CR users at different locations. This can be specially helpful in the study of cooperative techniques such as cooperative spectrum sensing, where the nodes of a DSA/CR network exchange sensing information (i.e., the channel state observed by each DSA/CR node) in order to provide a more reliable estimation of the real busy/idle state of the channel. As an example, let's consider a DSA/CR node blocked by a radio propagation obstacle (e.g., a building), which may misdetect a primary signal. Cooperation with other DSA/CR nodes could alleviate the problem. However, if the cooperating DSA/CR nodes are blocked by the same obstacle, they may experience similar SNR levels and observe the same channel state. In such a case, cooperation among these users would not provide significant gains. On the other hand, other DSA/CR nodes in better radio propagation conditions may experience higher SNR levels and detect the presence of the primary signal when it is active. The characterisation of the simultaneous observations of various DSA/CR users as a function of their locations and experienced SNRs can be of great utility in the study of cooperative DSA/CR techniques. In this context, this section extends the models of Section IV with additional considerations to characterise the concurrent observations of DSA/CR users at different locations.

Let's define the *reference location* of a spatial region under study as the location where the experienced SNR is maximum. Thus, by definition, the SNR Γ^* at the reference location satisfies the inequality $\Gamma^* \geq \Gamma$, where Γ represents the SNR experienced at any arbitrary location within the region under study. The previous inequality also implies that the average DC Ψ^* perceived at the reference location satisfies the condition $\Psi^* \geq \Psi$ for all the DC values Ψ observed in the area under study. Let's denote the state space of a primary radio channel as $\mathbb{S} = \{s_0, s_1\}$, where the s_0 and s_1 states indicate that the channel is observed as idle and busy, respectively. The instantaneous observation at any arbitrary location can be characterised in terms of the joint probability $P(s_i, s_j^*)$, with $i, j \in \{0, 1\}$, that the channel is simultaneously observed in state s_i at the selected arbitrary location and in state s_j at the reference location, or alternatively, in terms of the conditional probability $P(s_i \mid s_j^*)$ that the channel is observed in state s_i at the arbitrary location given that it has been observed in state s_j at the reference location. This probabilistic characterisation can be extended to any number of locations over the area under study by taking one location as a reference point (i.e., the location experiencing the highest SNR) and comparing, in pairs, with the rest of considered locations.

A. Joint and conditional probabilities

The analytical expressions of $P(s_i, s_j^*)$ and $P(s_i \mid s_j^*)$ for an arbitrary location can be derived as a function of the DC

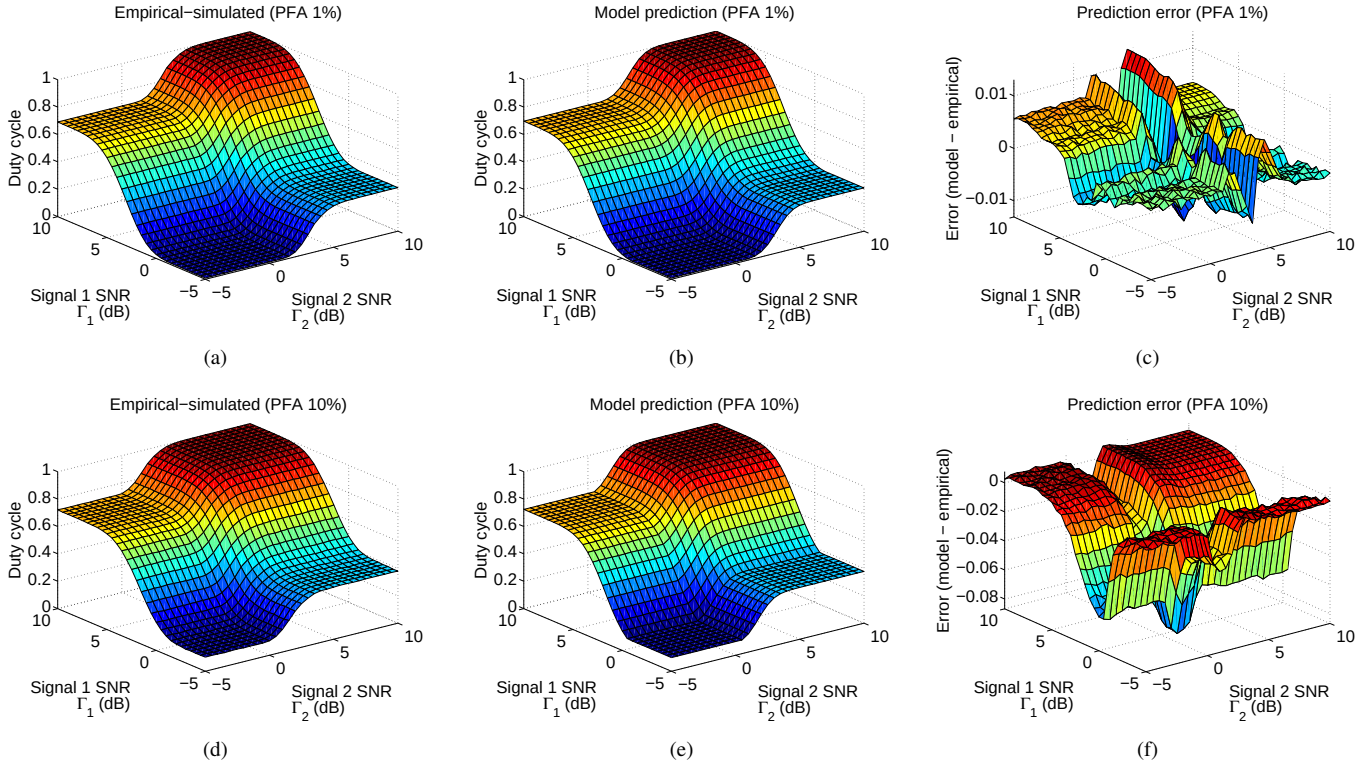

Fig. 6. Validation of the DC model for variable-power discontinuous transmitters: (a) empirical-simulated DC for P_{fa} = 1%, (b) DC model prediction for P_{fa} = 1%, (c) DC model prediction error for P_{fa} = 1%, (d) empirical-simulated DC for P_{fa} = 10%, (e) DC model prediction for P_{fa} = 10%, (f) DC model prediction error for P_{fa} = 10%.

value observed at the desired location (Ψ) and the DC value observed at the reference location (Ψ^*).

The set of conditional probabilities $P(s_i \,|\, s_j^*)$ can be derived as follows. When the channel is observed as idle at the reference location, this means that the channel is actually idle, or it is busy but the received power is below the decision threshold. In the latter case, the power received at any location whose receiving SNR is lower will also be below the decision threshold and the channel will also be observed as idle. However, there exists a probability P_{fa} that the channel is observed as busy because of noise samples above the threshold. Thus[5], $P(s_1 \,|\, s_0^*) = P_{fa}$ and its complementary probability is $P(s_0 \,|\, s_0^*) = 1 - P_{fa}$. On the other hand, when the channel is observed as busy at the reference location, this means that there has been a false alarm at the reference receiver, or the channel is actually busy and it has been received at the reference location with a power level above the decision threshold. In this case, the probability that the channel is observed as busy/idle at an arbitrary location depends not only on the probability of false alarm but also the experienced SNR Γ and its relation to the reference SNR Γ^*. The conditional probability $P(s_0 \,|\, s_1^*)$ can be derived by writing the probability $P(s_0)$ that the channel is observed as idle at the arbitrary location in the following form:

$$\begin{aligned} P(s_0) &= P(s_0 \,|\, s_0^*)P(s_0^*) + P(s_0 \,|\, s_1^*)P(s_1^*) \\ &= (1 - P_{fa})(1 - \Psi^*) + P(s_0 \,|\, s_1^*)\Psi^* = 1 - \Psi \end{aligned} \quad (12)$$

where $P(s_j^*)$ represents the probability that the channel is observed in state s_j at the reference location and it has been made use of the equivalence $P(s_0) = 1 - \Psi$. Solving (12) for the desired term yields:

$$P(s_0 \,|\, s_1^*) = \frac{1 - \Psi - (1 - P_{fa})(1 - \Psi^*)}{\Psi^*} \quad (13)$$

Following a similar procedure:

$$\begin{aligned} P(s_1) &= P(s_1 \,|\, s_0^*)P(s_0^*) + P(s_1 \,|\, s_1^*)P(s_1^*) \\ &= P_{fa}(1 - \Psi^*) + P(s_1 \,|\, s_1^*)\Psi^* = \Psi \end{aligned} \quad (14)$$

which yields:

$$P(s_1 \,|\, s_1^*) = \frac{\Psi - P_{fa}(1 - \Psi^*)}{\Psi^*} \quad (15)$$

The joint probabilities $P(s_i, s_j^*)$ can be obtained based on their conditional counterparts as $P(s_i, s_j^*) = P(s_i \,|\, s_j^*)P(s_j^*)$, where $P(s_0^*) = 1 - \Psi^*$ and $P(s_1^*) = \Psi^*$. Table I shows the entire set of joint and conditional probabilities. These expressions, combined with the analytical models of Section IV, can be employed to characterise not only the probability that a channel is observed as busy (DC) as a function of the DSA/CR user location and some basic primary signal parameters, but also the joint and conditional probabilities that the channel is observed in any of its states with respect to the simultaneous observation of other DSA/CR users.

[5]These equalities are *always* true *only* if the SNR at the reference location is higher. Otherwise, the event of observing the channel as idle at the reference location would not provide any information about the observation at other arbitrary locations with higher SNRs where the channel could be correctly observed as busy (the same applies to the other expressions in Table I).

TABLE I
PROBABILITIES OF SIMULTANEOUS OBSERVATIONS.

s_i	s_j^*	$P(s_i, s_j^*)$	$P(s_i \mid s_j^*)$
s_0	s_0^*	$(1-P_{fa})(1-\Psi^*)$	$1-P_{fa}$
s_1	s_0^*	$P_{fa}(1-\Psi^*)$	P_{fa}
s_0	s_1^*	$1-\Psi-(1-P_{fa})(1-\Psi^*)$	$\frac{1-\Psi-(1-P_{fa})(1-\Psi^*)}{\Psi^*}$
s_1	s_1^*	$\Psi-P_{fa}(1-\Psi^*)$	$\frac{\Psi-P_{fa}(1-\Psi^*)}{\Psi^*}$

B. Model validation

The validity of the expressions in Table I was assessed based on synchronised field measurements. As described in Section III, one measurement suite was placed in the outdoor high point (location 1 in Fig. 2), where the maximum experienced SNR was observed, while the second measurement suite was displaced along the rest of outdoor locations at the ground level (locations 3-12 in Fig. 2). This allowed the comparison of the occupancy patterns simultaneously perceived at various pairs of locations with different SNR levels.

The sequences of received powers were converted to sequences of busy/idle states by applying an energy detection method as mentioned in Section III. Based on a direct comparison of the sequences, the joint and conditional probabilities were extracted for each measured pair of locations. The obtained empirical results are shown in Figs. 7 and 8 along with the corresponding theoretical predictions, as a function of the SNR difference with respect to the reference location. The theoretical curves were obtained by first estimating the required signal parameters (μ_{S_k}, σ_{S_k}, α_k) and noise parameters (μ_N, σ_N) from the empirical data (as explained in Section IV-C), and then employing the corresponding analytical expressions presented in Section IV along with the expressions shown in Table I. As observed, there exists a nearly perfect agreement between the empirical results and theoretical predictions, which confirms the validity of the proposed modelling approach and highlights its capability to provide accurate predictions of the spectrum occupancy perceived in real environments.

VI. APPLICABILITY EXAMPLES

The models presented in Section IV and Section V are essentially theoretical and rely on closed-form expressions. As such, the developed models can be employed in analytical studies. However, the applicability of the models is not confined to analytical studies since other fields of application can be identified. This section presents two detailed examples to illustrate the practical applicability of the spectrum occupancy models developed in this work. The first example shows how the proposed modelling approaches can be combined with radio propagation models in order to provide a statistical characterisation of the spectrum occupancy perceived at various locations within a realistic environment, while the second example illustrates how they can be implemented and exploited in simulation tools[6].

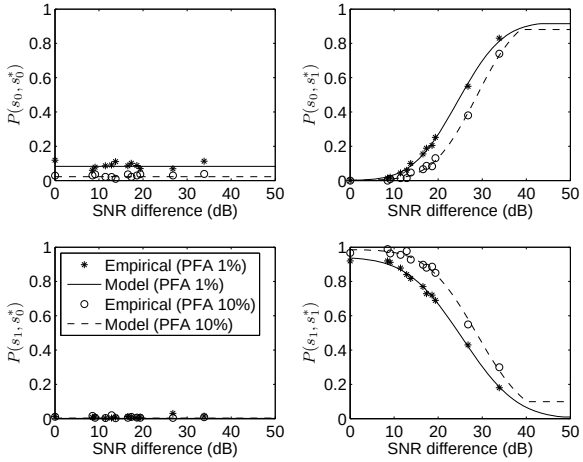

Fig. 7. Empirical validation of the joint probabilities.

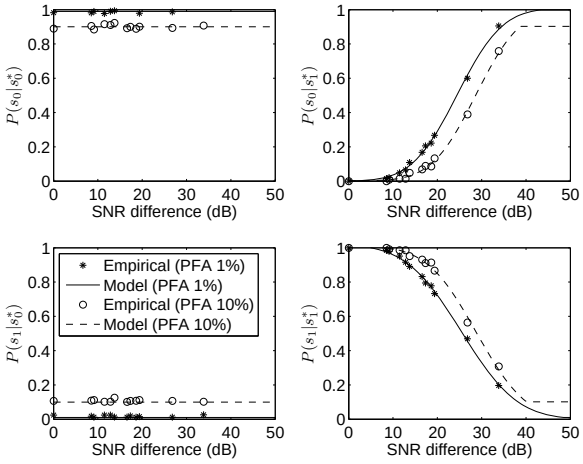

Fig. 8. Empirical validation of the conditional probabilities.

A. Prediction of spectrum occupancy perception

The behaviour and performance of a DSA/CR network depends on the spectrum occupancy perceived by each DSA/CR node in its local environment. The prediction of the spectrum occupancy perceived by DSA/CR users in different locations as a function of the surrounding radio propagation environment constitutes a valuable tool for the analysis, design, dimensioning and performance evaluation of DSA/CR systems.

1) Prediction approaches: A simple prediction method based on radio propagation models (frequently employed in the context of DSA/CR) is shown in Fig. 9(a). A radio propagation model is used to compute, based on a set of input

[6]While the results presented in Section VI-A are similar to some results presented in [49], the former are based on the more accurate models presented in Section IV-B while the latter are based on the preliminary models presented in [47]. The results in Section VI-B are new.

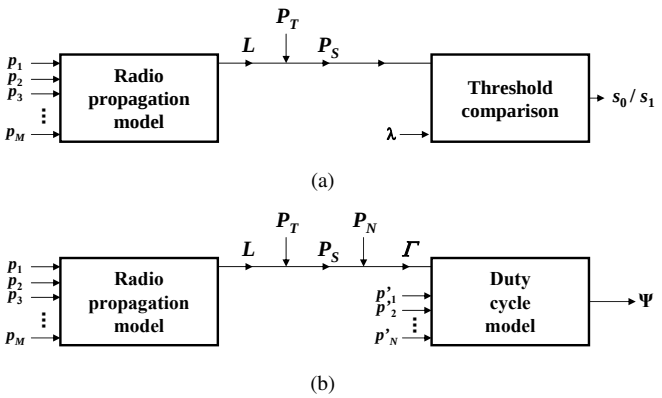

Fig. 9. Prediction of spectrum occupancy: (a) binary prediction approach, (b) probabilistic prediction approach.

parameters $\mathbf{p} = (p_1, p_2, \ldots, p_M)$ such as operating frequency, distance, etc., the path loss L between the primary transmitter and the locations of interest in the considered spatial region. The parameter set $\mathbf{p}$ required to estimate L is specific to the path loss model selected for the scenario under study. The primary signal powers P_S received at the locations of interest are obtained as $P_S(\mathrm{dBm}) = P_T(\mathrm{dBm}) - L(\mathrm{dB})$, where P_T is the primary transmission power. Assuming energy detection, the average power levels P_S predicted with the path loss model are compared to a decision threshold λ, thus providing a binary channel observation result (idle s_0, or busy s_1) for each analysed location. The main advantage of this approach is its simplicity. However, this method results in an oversimplified characterisation of the perceived spectrum occupancy where, for a particular location, the spectrum is observed either as always idle or always busy. In practice, radio propagation phenomena such as slow (shadowing) and fast (multipath) fading cause momentary signal fades, which may result in momentary signal misdetections, specially under sufficiently low SNR conditions (a case of particular interest for DSA/CR).

An alternative prediction approach is shown in Fig. 9(b), which combines radio propagation models and the spectrum occupancy models developed in this work [49]. As opposed to the binary prediction method mentioned above, the received P_S levels are not compared to a decision threshold, but converted to SNR values $\Gamma(\mathrm{dB}) = P_S(\mathrm{dBm}) - P_N(\mathrm{dBm})$, where P_N is the DSA/CR receiver's noise, given by $P_N(\mathrm{dBm}) = -174\mathrm{dBm/Hz} + 10\log_{10} B(\mathrm{Hz}) + \mathrm{NF(dB)}$, with $-174\mathrm{dBm/Hz}$ being the thermal noise power spectral density at 290K, B the radio bandwidth of the sensed channel, and NF the noise figure of the DSA/CR terminal. The resulting SNR values Γ are then fed, along with an additional set of input parameters $\mathbf{p}' = (p'_1, \ldots, p'_N)$, to the DC model, which outputs an estimation Ψ of the DC perceived by the DSA/CR users at the considered locations of interest. The DC model, in its most general form, is given by (11) and the involved variables and parameters constitute the input vector $\mathbf{p}'$.

The main advantage of the probabilistic approach is its capability to include the effects of signal and noise power variations on the predicted spectrum occupancy perception. The instantaneous values of signal and noise power experienced at various sensing events may suffer some fluctuations around the mean values μ_S and μ_N, respectively. The effective signal power P_S may vary due to the primary transmission power pattern along with shadowing and multipath fading effects. The effective noise power P_N may vary due to finite sensing times, which may not be long enough to average the instantaneous oscillations of noise, or other reasons such as temperature variations. The fluctuations of the signal and noise powers are included by means of the σ_S and σ_N parameters (note that these are some of the input parameters of vector $\mathbf{p}'$ in Fig. 9). The values of σ_S and σ_N can be estimated by means of appropriate radio propagation models, simulation/radio planning tools or field measurements. Table II shows some examples of σ_S and σ_N for various bands, which have been derived from field measurements. Note that the received signal is always affected by the receiver's noise and, as a result, $\sigma_S > \sigma_N$. The employed spectrum analyser sweeps at an average speed of 25 ms/MHz, which results in the effective channel observation (sensing) times shown in Table II. As it can be appreciated, there is a direct relation between the effective sensing time and the resulting σ_N. The trend is not so well-defined for σ_S, which depends on particular technology-specific power patterns and the channel fading properties at various frequencies.

TABLE II
EXPERIMENTAL VALUES OF σ_S AND σ_N.

Band	B (Hz)	Sensing (ms)	σ_S (dB)	σ_N (dB)
TV	$8 \cdot 10^6$	200	0.5252	0.1679
UMTS	$5 \cdot 10^6$	125	0.4138	0.2093
DAB	$1.7 \cdot 10^6$	42.5	0.8298	0.3640
GSM/DCS	$200 \cdot 10^3$	5	1.6421	0.8921
TETRA	$25 \cdot 10^3$	0.625	2.0469	1.3624

2) Considered scenario and propagation models: To illustrate the prediction approaches of Section VI-A1, a generic urban environment is considered where buildings of height h_r = 40 m are deployed following a uniform layout with inter-building separation b = 40 m and street width w = 20 m as shown in Fig. 10. The area under study is composed of a grid of 5×5 buildings. A TV transmitter with height h_b = 50 m, operating at a frequency $f = 800$ MHz and transmission power P_T = 60 dBm, is located d = 4.8 km apart. Within this scenario, DSA/CR terminals using energy detection with a target P_{fa} = 0.01, NF = 8.6 dB, and antenna height $h_m = 2$ m, are located at the center of building rooftops (height is $h_r + h_m$), at the ground level between buildings (height is h_m), or inside buildings (height is $n \cdot h + h_m$, with n = 3 being the floor number and $h = 3$ m/floor). These locations represent scenarios of practical interest and embrace a wide range of receiving conditions, from direct line-of-sight at rooftops to severely blocked and faded signals at the ground level and inside buildings.

For computation purposes, the area under study is here represented by a matrix of 100×100 elements, each of which represents a possible location for DSA/CR users. The state of

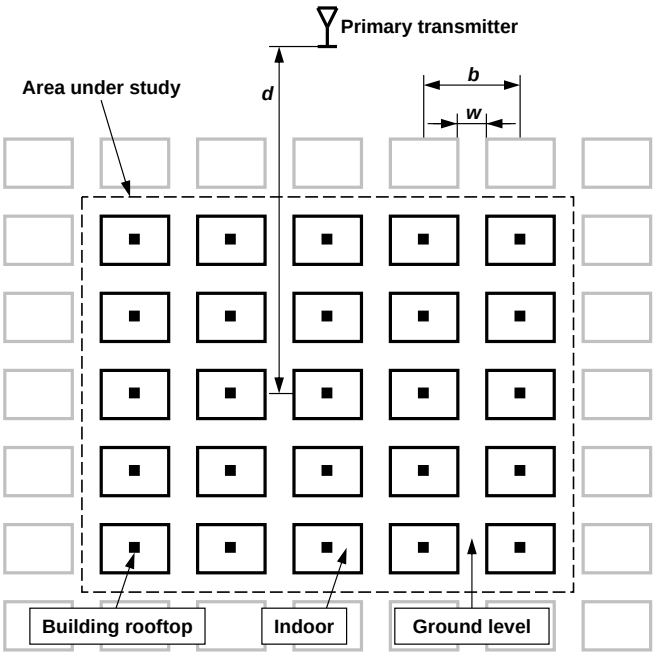

Fig. 10. Considered scenario.

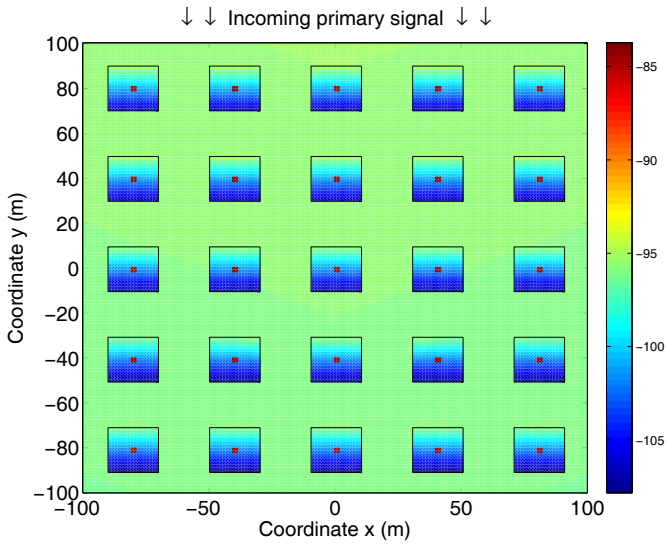

Fig. 11. Received primary signal power $P_S(\mathrm{dBm})$.

each element (i.e., possible location) is computed individually based on the developed models.

The average primary signal power received at every location is computed based on the Okumura-Hata model [50], [51] (including the Hata's correction factor for open areas [51, (19-20)]) for DSA/CR users in building rooftops, the COST231 Walfisch-Ikegami model [52] for DSA/CR users at the ground level, and the building penetration loss model for non-line-of-sight conditions described in [52] for indoor DSA/CR users. Signal and noise power fluctuations are characterised by σ_S = 0.5252 dB and σ_N = 0.1679 dB, respectively (see Table II).

3) Numerical results: Fig. 11 shows the primary signal power P_S(dBm) received at various locations in the area under study, based on the radio propagation models mentioned in Section VI-A2. As it can be appreciated, the highest power level is observed at rooftops, with significantly lower powers received at the ground level (around 10 dB lower) and inside buildings (around 20 dB lower). This suggests that DSA/CR users within the same region may experience quite dissimilar perceptions depending on their particular locations and propagation conditions.

Fig. 12 shows the perceived spectrum occupancy pattern as predicted by the method of Fig. 9(a). White and grey colours indicate that the primary channel is observed as busy and idle, respectively, at the corresponding locations. According to the predicted pattern, the TV channel is always observed as busy (idle) at rooftops (indoor locations), where the highest (lowest) power levels are in general observed. At the ground level, different cases are observed depending on the distance from the primary transmitter. However, it is worth highlighting that this prediction approach indicates the existence of a hard limit such that the primary channel is always observed as busy at locations slightly above, and idle at locations slightly below, which provides not only an excessively simplistic, but also unrealistic characterisation of the perceived spectrum occupancy pattern.

Fig. 13 shows the perceived spectrum occupancy pattern predicted by the method of Fig. 9(b). Comparing with Fig. 12, it can be observed that both prediction approaches agree for locations at building rooftops (the channel is observed as busy with probability one, i.e., always) and indoor environments (the channel is observed as busy with probability zero, i.e., never), where the highest and lowest received powers are observed, respectively. The differences between both approaches are observed in the spectrum occupancy perception predicted at the ground level. As opposed to the binary prediction method, where a hard borderline is observed, the prediction method based on the developed DC models provides a more sophisticated characterisation in terms of the probability that the spectrum is observed as busy, which increases progressively as the considered location approaches the primary transmitter (without observing any abrupt transitions).

This example illustrates how the developed spectrum occupancy models can be combined with radio propagation models in a probabilistic prediction approach to provide a sophisticated characterisation of the perceived spectrum occupancy, as a function of the considered location and surrounding radio propagation scenario.

B. Snapshot-based simulations

Another illustrative example of the applicability of the models developed in this work is the development of innovative and improved simulation methods. The models of Section IV can be used to determine the average DC perceived at every location inside the simulation scenario as illustrated in Fig. 13. As the DC represents the probability that the primary channel is observed as busy, the local decisions of DSA/CR terminals can be obtained by comparing the DC values Ψ computed at their locations with a random value ξ drawn from a uniform distribution $U(0,1)$. If $\xi \leq \Psi$, then the DSA/CR

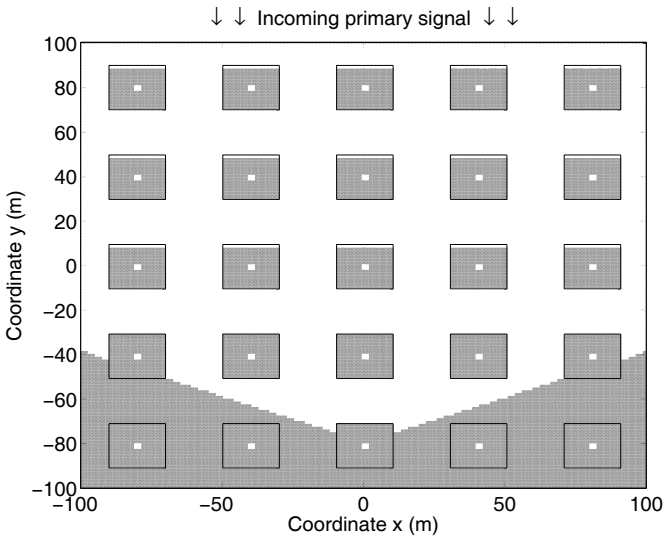

Fig. 12. Binary spectrum occupancy pattern.

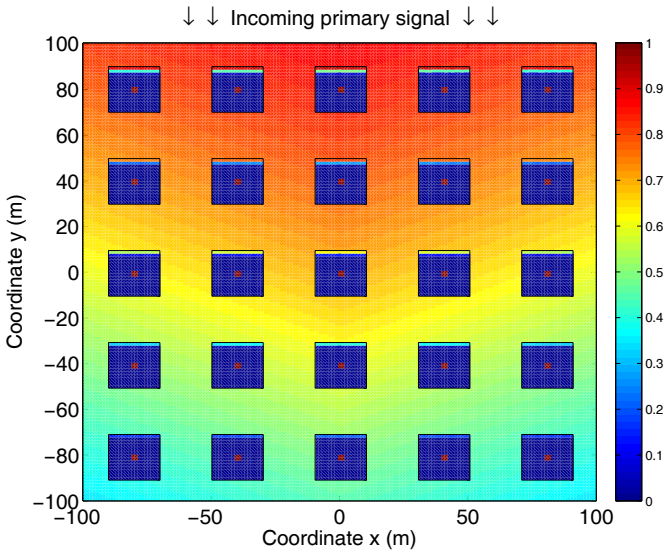

Fig. 13. Probabilistic spectrum occupancy pattern.

terminal observes the channel as busy. Otherwise, the channel is observed as idle. This procedure can be repeated to generate several simulation snapshots.

While the previous simulation approach provides the right average DC in the long-term, the simultaneous observations of various DSA/CR users at particular time instants (i.e., in a snapshot) are independent of each other. This simulation approach can be refined by additionally taking into account the expressions shown in Table I in order to characterise the simultaneous observations. For each snapshot, the channel state s_j^* observed at the reference (maximum SNR) location is first determined in a random way as mentioned above. The instantaneous channel state s_i observed in the rest of locations is then determined as follows. When the channel is observed as idle at the reference location ($s_j^* = s_0^*$), the rest of locations may observe the channel as busy with probability $P(s_1 \,|\, s_0^*) = P_{fa}$ and idle with probability $P(s_0 \,|\, s_0^*) = 1 - P_{fa}$. On the other hand, when the channel is perceived as busy at the reference location ($s_j^* = s_1^*$), the rest of locations may observe the channel as busy with probability $P(s_1 \,|\, s_1^*) = [\Psi - P_{fa}(1-\Psi^*)]/\Psi^*$ and idle with probability $P(s_0 \,|\, s_1^*) = [1-\Psi-(1-P_{fa})(1-\Psi^*)]/\Psi^*$. These probabilities can be used to determine the channel states s_i observed in other locations based on random numbers $\xi \sim U(0,1)$. This procedure can be repeated to generate snapshots that reproduce not only the average DC values in the long-term, but also the simultaneous observations at various locations.

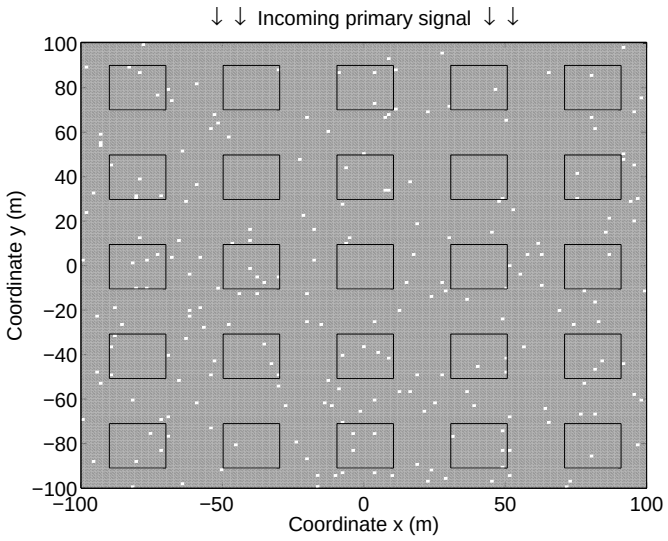

Fig. 14. Random simulation snapshot when the channel is observed as idle at the reference location.

As an illustrative example, Figs. 14 and 15 show some random simulation snapshots generated with the aforementioned simulation method, for the scenario considered in Section VI-A. The reference (highest SNR) location in this scenario corresponds to the rooftop in the coordinate ($x = 0m, y = 80m$). White and grey colours indicate that the primary channel is observed as busy and idle, respectively, at the corresponding locations. When the channel is idle at the reference location (Fig. 14), it is also observed as idle (grey) in most locations except in some particular cases where it is observed as busy (white) as a result of some false alarms. On the other hand, when the channel is perceived as busy at the reference location (Fig. 15), the rest of locations may observe the channel as busy (white) or idle (grey) depending on the particular user location and the corresponding conditional probabilities. In general, in areas close to the primary transmitter (top of Fig. 15) the probability to observe the channel as busy (white) is higher and as a result there is a higher number of locations where it is detected in such state. This example illustrates how the proposed models can be combined and employed in the implementation and development of simulation tools for DSA/CR research.

VII. Conclusions

Realistic and accurate spectrum occupancy models constitute a valuable tool in the analysis, design and simulation of

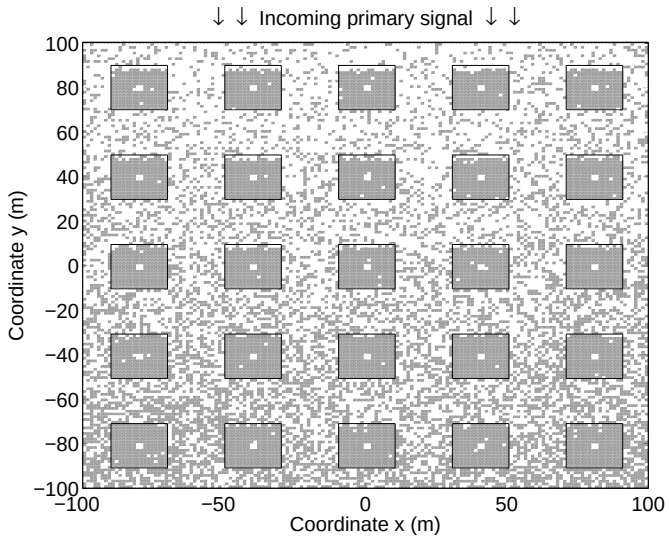

Fig. 15. Random simulation snapshot when the channel is observed as busy at the reference location.

DSA/CR networks. This work has addressed the problem of modelling spectrum usage in the spatial domain by introducing a novel set of models that describe the average spectrum occupancy level (expressed in terms of the DC) perceived by DSA/CR users at any arbitrary location based on the knowledge of some simple primary signal parameters. An extension has also been proposed in order to characterise not only the average occupancy perception but also the simultaneous observations of various DSA/CR users. The validity and correctness of the proposed modelling approaches have been evaluated and corroborated with extensive empirical data from a multi-band spectrum measurement campaign, performed with an advanced measurement platform. Some illustrative examples of the potential applicability of the developed models have been presented and discussed as well.

APPENDIX
ESTIMATION OF MODEL PARAMETERS

This appendix discusses how the model parameters (primary activity factor and signal- and noise-related parameters) can be estimated in practical scenarios.

The activity factor of an unknown primary transmitter and the signal power parameters of the models could be estimated from field measurements performed under sufficiently high SNR conditions (e.g., in a location sufficiently close to the primary transmitter). As discussed at the beginning of Section IV, the duty cycle observed in such a case would provide an accurate estimation of the primary activity factor. Moreover, under sufficiently high SNR conditions there would be a wide range of values for the detection threshold that would enable an easy separation of signal and noise measurement samples (based on their power levels). The signal samples could then be processed individually in order to estimate the signal-related parameters of the models. This approach has been employed in the experimental part of this work and a nearly perfect match between theoretical and empirical results has been observed. Wherever field measurements are not feasible, the model parameters could be estimated based on radio planning tools or simulators.

The estimation of the noise parameters, however, is more problematic in practice and a more critical aspect. In the literature, the noise statistics of the receiver have frequently been assumed to be constant and known. However, in practice, the noise floor of a receiver depends not only on its circuitry but also on random parameters such as temperature or external noise sources that may increase the effective noise (out-of-band transmissions, ambient noise or man-made noise), which may also change over time [53]. All these phenomena have an impact on the effective noise floor and consequently on the spectrum occupancy observed by DSA/CR users (a more detailed discussion on noise sources and their impact on the observed spectrum occupancy is provided in [45]). The noise floor of a receiver could be determined in several ways. For example, it could be estimated from measurements on channels that are known to be idle. However, this approach has some drawbacks since harmonics, intermodulation products or other signal components resulting from non-linear effects may be present in idle channels; moreover, the estimated noise floor may not be useful for detection in other channels given the frequency-dependent nature of some noise sources. Another option would be a hardware design where the RF front-end can be switched between the antenna (for transmission) and a matched load (for noise estimation). However, this approach also has some drawbacks since some signal components might still be detected through the matched load, and some other external noise sources that are detected through the antenna would not be included in the estimated noise floor. To overcome these issues, more sophisticated methods have been proposed. In [54] a method to estimate flat or non-flat noise floor in the presence of unknown signals is proposed based on the use of morphological image processing operations. Information theoretic criteria relying on spectrum sensing methods based on Akaike's Information Criterion (AIC) or Minimum Description Length (MDL) have been proposed in [55]. Another noise power estimation method is proposed in [56] assuming perfect sensing during long sensing periods. More recently, other methods for noise estimation in the presence of signals have been proposed in [57]–[59] based on a median forward consecutive mean excision (MED-FCME) method and some variations thereof; their main advantage is the ability to estimate the noise floor directly from the signal while simultaneously performing regular measurements, and to react rapidly to changes in the noise floor.

REFERENCES

[1] S. Haykin, "Cognitive radio: Brain-empowered wireless communications," *IEEE Journal on Selected Areas in Comms.*, vol. 23, no. 2, pp. 201–220, Feb. 2005.
[2] J. Mitola, *Cognitive Radio Architecture*. Wiley, Oct. 2006.
[3] M. López-Benítez, "Cognitive radio," in *Heterogeneous cellular networks: Theory, simulation and deployment*. Cambridge University Press, 2013, ch. 13, pp. 383–425.
[4] I. F. Akyildiz, W.-Y. Lee, M. C. Vuran, and S. Mohanty, "NeXt generation/dynamic spectrum access/cognitive radio wireless networks: A survey," *Computer Networks*, vol. 50, no. 13, pp. 2127–2159, Sep. 2006.

[5] Q. Zhao and A. Swami, "A survey of dynamic spectrum access: signal processing and networking perspectives," in *Proc. IEEE Int'l. Conf. Acoustics, Speech and Signal Proc. (ICASSP 2007)*, vol. 4, Apr. 2007, pp. IV/1349–IV/1352.

[6] Q. Zhao and B. M. Sadler, "A survey of dynamic spectrum access," *IEEE Sig. Proc. Mag.*, vol. 24, no. 3, pp. 79–89, 2007.

[7] M. M. Buddhikot, "Understanding dynamic spectrum access: Taxonomy, models and challenges," in *Proc. 2nd IEEE Int'l. Symp. Dyn. Spec. Access Networks (DySPAN 2007)*, Apr. 2007, pp. 649–663.

[8] M. A. McHenry *et al.*, "Spectrum occupancy measurements," Shared Spectrum Company, Tech. Rep., Jan 2004 - Aug 2005, available at: http://www.sharedspectrum.com.

[9] R. I. C. Chiang, G. B. Rowe, and K. W. Sowerby, "A quantitative analysis of spectral occupancy measurements for cognitive radio," in *Proc. IEEE 65th Vehic. Tech. Conf. (VTC 2007 Spring)*, Apr. 2007, pp. 3016–3020.

[10] M. Wellens, J. Wu, and P. Mähönen, "Evaluation of spectrum occupancy in indoor and outdoor scenario in the context of cognitive radio," in *Proc. 2nd Int'l. Conf. Cog. Radio Oriented Wireless Netws. & Comms. (CrownCom 2007)*, Aug. 2007.

[11] M. H. Islam *et al.*, "Spectrum survey in Singapore: Occupancy measurements and analyses," in *Proc. 3rd Int'l. Conf. Cog. Radio Oriented Wireless Netws. and Comms. (CrownCom 2008)*, May 2008, pp. 1–7.

[12] M. López-Benítez, A. Umbert, and F. Casadevall, "Evaluation of spectrum occupancy in Spain for cognitive radio applications," in *Proc. IEEE 69th Vehic. Tech. Conf. (VTC 2009 Spring)*, Apr. 2009.

[13] M. López-Benítez, F. Casadevall, A. Umbert, J. Pérez-Romero, J. Palicot, C. Moy, and R. Hachemani, "Spectral occupation measurements and blind standard recognition sensor for cognitive radio networks," in *Proc. 4th Int'l. Conf. Cog. Radio Oriented Wireless Netws. and Comms. (CrownCom 2009)*, Jun. 2009, pp. 1–9.

[14] K. A. Qaraqe, H. Celebi, A. Gorcin, A. El-Saigh, H. Arslan, and M.-S. Alouini, "Empirical results for wideband multidimensional spectrum usage," in *Proc. IEEE 20th Int'l. Symp. Pers., Indoor and Mobile Radio Comms. (PIMRC 2009)*, Sep. 2009, pp. 1262–1266.

[15] A. Martian, I. Marcu, and I. Marghescu, "Spectrum occupancy in an urban environment: A cognitive radio approach," in *Proc. 6th Adv. Int'l. Conf. Telecomms. (AICT 2010)*, May 2010, pp. 25–29.

[16] R. Schiphorst and C. H. Slump, "Evaluation of spectrum occupancy in Amsterdam using mobile monitoring vehicles," in *Proc. IEEE 71st Vehic. Tech. Conf. (VTC Spring 2010)*, May 2010, pp. 1–5.

[17] V. Valenta, R. Maršálek, G. Baudoin, M. Villegas, M. Suarez, and F. Robert, "Survey on spectrum utilization in Europe: Measurements, analyses and observations," in *Proc. Fifth Int'l. Conf. Cog. Radio Oriented Wireless Netws. & Comms. (CrownCom 2010)*, Jun. 2010, pp. 1–5.

[18] M. López-Benítez and F. Casadevall, "Spectrum usage models for the analysis, design and simulation of cognitive radio networks," in *Cognitive radio and its application for next generation cellular and wireless networks*. Springer, 2012, ch. 2, pp. 27–73.

[19] X. Hong, C.-X. Wang, H.-H. Chen, and Y. Zhang, "Secondary spectrum access networks: Recent developments on the spatial models," *IEEE Vehic. Tech. Mag.*, vol. 4, no. 2, pp. 36–43, Jun. 2009.

[20] J. Li, S. Li, F. Zhao, and R. Du, "Co-channel interference modeling in cognitive wireless networks," *IEEE Trans. Commun.*, vol. 62, no. 9, pp. 3114–3128, Sep. 2014.

[21] L. Bedogni, A. Trotta, and M. D. Felice, "On 3-dimensional spectrum sharing for TV white and gray space networks," in *Proc. IEEE Int'l. Symp. World of Wireless, Mobile and Multimedia Networks (WoWMoM 2015)*, Jun. 2015, pp. 1–8.

[22] N. Hoven and A. Sahai, "Power scaling for cognitive radio," in *Proc. Int'l. Conf. Wireless Networks, Comms. and Mobile Computing (WNCMC)*, Jun. 2005, pp. 250–255.

[23] M. Timmers, S. Pollin, A. Dejonghe, A. Bahai, L. van der Perre, and F. Catthoor, "Accumulative interference modeling for distributed cognitive radio networks," *Journal of Comms.*, vol. 4, no. 3, pp. 175–185, Apr. 2009.

[24] R. Menon, R. M. Buehrer, and J. Reed, "Outage probability based comparison of underlay and overlay spectrum sharing techniques," in *Proc. First IEEE Int'l. Symp. Dyn. Spec. Access Networks (DySPAN 2005)*, Nov. 2005, pp. 101–109.

[25] T. Kamakaris, D. Kivanc-Tureli, and U. Tureli, "Interference model for cognitive coexistence in cellular systems," in *Proc. IEEE Global Telecomms. Conf. (GLOBECOM 2007)*, Nov. 2007, pp. 4175–4179.

[26] R. S. Dhillon and T. X. Brown, "Models for analyzing cognitive radio interference to wireless microphones in TV bands," in *Proc. 3rd IEEE Symp. Dyn. Spec. Access Networks (DySPAN 2008)*, Oct. 2008, pp. 1–10.

[27] X. Hong, C.-X. Wang, and J. S. Thompson, "Interference modeling of cognitive radio networks," in *Proc. IEEE Vehic. Tech. Conf. (VTC 2008 Spring)*, May 2008, pp. 1851–1855.

[28] R. Menon, R. Buehrer, and J. Reed, "On the impact of dynamic spectrum sharing techniques on legacy radio systems," *IEEE Trans. Wireless Comms.*, vol. 7, no. 11, pp. 4198–4207, Nov. 2008.

[29] Z. Chen, C.-X. Wang, X. Hong, J. Thompson, S. Vorobyov, and X. Ge, "Interference modeling for cognitive radio networks with power or contention control," in *Proc. IEEE Wireless Comms. and Netw. Conf. (WCNC 2010)*, Apr. 2010, pp. 1–6.

[30] D. Willkomm, S. Machiraju, J. Bolot, and A. Wolisz, "Primary users in cellular networks: A large-scale measurement study," in *Proc. 3rd IEEE Int'l. Symp. Dyn. Spec. Access Networks (DySPAN 2008)*, Oct. 2008, pp. 1–11.

[31] O. Holland, P. Cordier, M. Muck, L. Mazet, C. Klöck, and T. Renk, "Spectrum power measurements in 2G and 3G cellular phone bands during the 2006 Football World Cup in Germany," in *Proc. 2nd IEEE Int'l. Symp. Dyn. Spec. Access Networks (DySPAN 2007)*, Apr. 2007, pp. 575–578.

[32] T. Renk, C. Kloeck, F. K. Jondral, P. Cordier, O. Holland, and F. Negredo, "Spectrum measurements supporting reconfiguration in heterogeneous networks," in *Proc. 16th IST Mobile and Wireless Comms. Summit (IST Mobile Summit 2007)*, Jul. 2007, pp. 1–5.

[33] T. Kamakaris, M. M. Buddhikot, and R. Iyer, "A case for coordinated dynamic spectrum access in cellular networks," in *Proc. First IEEE Int'l. Symp. Dyn. Spec. Access Networks (DySPAN 2005)*, Nov. 2005, pp. 289–298.

[34] J. Riihijärvi, P. Mähönen, M. Wellens, and M. Gordziel, "Characterization and modelling of spectrum for dynamic spectrum access with spatial statistics and random fields," in *Proc. Int'l. W'shop. Cog. Radios & Netws. (CRNETS 2008)*, Sep. 2008.

[35] M. Wellens, J. Riihijärvi, M. Gordziel, and P. Mähönen, "Spatial statistics of spectrum usage: From measurements to spectrum models," in *Proc. IEEE Int'l. Conf. Comms. (ICC 2009)*, Jun. 2009.

[36] M. Wellens, J. Riihijärvi, and P. Mähönen, "Spatial statistics and models of spectrum use," *Computer Comms.*, vol. 32, no. 18, pp. 1998–2011, Dec. 2009.

[37] B. Sayrac, L. Gueguen, C. C. Trang, and A. M. G. Serrano, "Point-process based localization of primary users in collaborative dynamic spectrum access," in *Proc. 20th Int'l. Conf. Telecomms. (ICT 2013)*, May 2013, pp. 1–5.

[38] J. Riihijärvi, J. Nasreddine, and P. Mähönen, "Impact of primary user activity patterns on spatial spectrum reuse opportunities," in *Proc. European Wireless Conf. (EW 2010)*, Apr. 2010, pp. 962–968.

[39] L. Liu, H. Li, and Z. Han, "Sampling spectrum occupancy data over random fields: A matrix completion approach," in *Proc. IEEE Int'l. Conf. Comms. (ICC 2012)*, Jun. 2012, pp. 1487–1491.

[40] S. Yin and S. Li, "Spatio-temporal characterization for mobile service usage based on spectrum measurement," in *Proc. IEEE Int'l. Conf. Comms. (ICC 2014)*, Jun. 2014, pp. 1645–1650.

[41] Y. Chen and H.-S. Oh, "A survey of measurement-based spectrum occupancy modeling for cognitive radios," *IEEE Comms. Surveys & Tutorials*, Oct. 2014, in press.

[42] H. Urkowitz, "Energy detection of unknown deterministic signals," *Proc. IEEE*, vol. 55, no. 4, pp. 523–531, Apr. 1967.

[43] M. López-Benítez and F. Casadevall, "A radio spectrum measurement platform for spectrum surveying in cognitive radio," in *Proc. 7th Int'l. ICST Conf. Testbeds and Research Infrastructures for the Development of Networks and Communities (TridentCom 2011)*, Apr. 2011, pp. 1–16.

[44] ——, "Methodological aspects of spectrum occupancy evaluation in the context of cognitive radio," *European Trans. Telecomms.*, vol. 21, no. 8, pp. 680–693, Dec. 2010.

[45] ——, "On the spectrum occupancy perception of cognitive radio terminals in realistic scenarios," in *Proc. 2nd Int'l. Workshop Cognitive Inf. Proc. (CIP 2010)*, Jun. 2010, pp. 1–6.

[46] M. López-Benítez and F. Casadevall, "Improved energy detection spectrum sensing for cognitive radio," *IET Communications*, vol. 6, no. 8, pp. 785–796, May 2012.

[47] M. López-Benítez and F. Casadevall, "Spatial duty cycle model for cognitive radio," in *Proc. 21st Annual IEEE Int'l. Symp. Pers., Indoor and Mobile Radio Comms. (PIMRC 2010)*, Sep. 2010, pp. 1631–1636.

[48] M. Abramowitz and I. A. Stegun, *Handbook of mathematical functions with formulas, graphs, and mathematical tables*. Dover, 1972.

[49] M. López-Benítez and F. Casadevall, "Statistical prediction of spectrum occupancy perception in dynamic spectrum access networks," in *Proc. IEEE Int'l. Conf. Comms. (ICC 2011)*, Jun. 2011.

[50] Y. Okumura, E. Ohmori, T. Kawano, and K. Fukuda, "Field strength and its variability in VHF and UHF land-mobile radio service," *Review of the Electrical Comms. Lab.*, vol. 16, no. 9-10, pp. 825–873, Sep. 1968.
[51] M. Hata, "Empirical formula for propagation loss in land mobile radio services," *IEEE Trans. Vehic. Tech.*, vol. VT-29, no. 3, pp. 317–325, Aug. 1980.
[52] D. J. Cichon and T. Kürner, "Propagation prediction models (Digital mobile radio towards future generation systems, chapter 4)," COST231, Tech. Rep., Nov. 1998.
[53] D. Torrieri, "The radiometer and its practical implementation," in *Proc. IEEE Mil. Comms. Conf. (MILCOM 2010)*, Nov. 2010, pp. 304–310.
[54] M. J. Ready, M. L. Downey, and L. J. Corbalis, "Automatic noise floor spectrum estimation in the presence of signals," in *Proc. 31st Asilomar Conf. Signal, Systems & Computers (ASILOMAR 1997)*, vol. 1, Nov. 1997, pp. 877–881.
[55] S. Liu, J. Shen, R. Zhang, Z. Zhang, and Y. Liu, "Information theoretic criterion-based spectrum sensing for cognitive radio," *IET Communications*, vol. 2, no. 6, pp. 753–762, Jul. 2008.
[56] A. Mariani, A. Giorgetti, and M. Chiani, "Effects of noise power estimation on energy detection for cognitive radio applications," *IEEE Trans. Comms.*, vol. 59, no. 12, pp. 3410–3420, Dec. 2011.
[57] J. Lehtomäki, R. Vuohtoniemi, and K. Umebayashi, "On the measurement of duty cycle and channel occupancy rate," *IEEE J. Sel. Areas Commun.*, vol. 31, no. 11, pp. 2555–2565, Nov. 2013.
[58] J. J. Lehtomäki, R. Vuohtoniemi, K. Umebayashi, and J.-P. Mäkelä, "Energy detection based estimation of channel occupancy rate with adaptive noise estimation," *IEICE Trans. Commun.*, vol. E95-B, no. 4, pp. 1076–1084, Apr. 2012.
[59] K. Umebayashi, R. Takagi, N. Ioroi, J. Lehtomäki, and Y. Suzuki, "Duty cycle and noise floor estimation with Welch FFT for spectrum usage measurements," in *Proc. 9th Int'l. Conf. Cog. Radio Oriented Wireless Netws. and Comms. (CrownCom 2014)*, Jun. 1997, pp. 73–78.

Miguel López-Benítez (S'08, M'12) received the BSc (2003) and MSc (2006) degrees in Communications Engineering (First-Class Honours) from Miguel Hernández University (UMH), Elche, Spain, and the PhD degree (2011) in Communications Engineering from the Department of Signal Theory and Communications (TSC) of the Technical University of Catalonia (UPC), Barcelona, Spain.

From 2011 to 2013 he was a Research Fellow in the Centre for Communication Systems Research, University of Surrey, United Kingdom. Since 2013 he has been a Lecturer (Assistant Professor) in the Department of Electrical Engineering and Electronics, University of Liverpool, United Kingdom.

His research interests include the field of mobile radio communication systems, with special emphasis on radio resource management, heterogeneous wireless systems, quality of service provisioning, spectrum modelling and opportunistic/dynamic spectrum access in cognitive radio networks. He was involved in the European-funded projects AROMA, NEWCOM++, FARAMIR, QoSMOS and CoRaSat along with Spanish projects COGNOS and ARCO. He has co-authored 3 book chapters and more than 50 papers in refereed journals and recognised conferences. He was a member of the Organising Committees for the IEEE WCNC International Workshop on Smart Spectrum (IWSS 2015 & IWSS 2016). He has served as a TPC for several IEEE conferences and as a reviewer for IEEE journals and conferences.

Dr. López-Benítez was the recipient of the 2003 and 2006 University Education National Awards to the best national academic records by the Spanish Ministry of Education and Science as well as some other distinctions from the Spanish professional association of telecommunication engineers. His MSc thesis received the France Telecom Foundation Special Award 2006 (in the context of the 5th Archimedes University Competition organised by the Spanish Ministry of Education and Science). He received a full PhD scholarship from the Spanish Ministry of Education and Science (ranked 1st in the Electronics and Telecommunications area) and the 2011 Outstanding PhD Thesis Award by the Department of Signal Theory and Communications at UPC. He was shortlisted as a finalist for the IET Innovation Awards 2012 in the category of Telecommunications. He received the Best Tutorial Paper Award 2014 from the Communications Society of the Institute of Electronics, Information and Communication Engineers (IEICE), and the IEEE Access Reviewer of the Month July 2015 Award from IEEE. For more details, please visit http://www.lopezbenitez.es.

Fernando Casadevall (M'87) received the Engineer (1977) and Doctor Engineer (1983) degrees in telecommunications engineering from Universitat Politècnica de Catalunya (UPC), Barcelona, Spain.

In 1978, he joined UPC, where he was an Associate Professor from 1983 to 1991. He is currently a Full Professor with the Department of Signal Theory and Communications, UPC. After graduation, he was concerned with equalization techniques for digital fiber-optic systems. He has also been working in the field of digital communications, with particular emphasis on digital radio and its performance under multipath propagation conditions. Over the last 20 years, he has been mainly concerned with the performance analysis and development of digital mobile radio systems. He has published around 150 technical papers in both international conferences and magazines, most of them corresponding to IEEE publications. His particular research interests include cellular and personal communication systems, cognitive radio issues, radio resource management techniques, transceiver design (including software radio techniques). Currently he is also involved in network virtualization and SDN techniques. During the last 20 years, he has participated in more than 30 research projects funded by both public and private organizations. In particular, he has actively participated in 15 research projects funded by the European Commission, being the Project Manager for three of them: Advanced Radio Resource management fOr Wireless Systems (ARROWS), Evolutionary Strategies for Radio Resource Management in Cellular Heterogeneous Networks (EVEREST), and Advanced Resource Management Solutions for Future All IP Heterogeneous Mobile Radio Environments (AROMA) (see http://www.gcr.tsc.upc.edu for details).

Prof. Casadevall has been a Technical Program Committee Member for different international IEEE supported conferences and a Reviewer for several IEEE magazines. From October 1992 to January 1996, he was in charge of the Information Technology Area, National Agency for Evaluation and Forecasting (Spanish National Research Council).